



## The influence of geometry on the TiO<sub>2</sub> nano-catalytic performance

Hassan Koohestani<sup>a</sup>, Sayed Khatiboleslam Sadrnezhaad<sup>a,\*</sup>

<sup>a</sup> Department of Materials Science and Engineering, Sharif University of Technology, Tehran, Iran

\*sadrnezh@sharif.edu

**Abstract:** Geometry affects photocatalytic behavior of TiO<sub>2</sub> nanometric samples. In this research, powder, fiber, film and network-shaped TiO<sub>2</sub> nanocatalysts were produced by using different templates. The products were characterized by x-ray diffraction (XRD), scanning electron microscopy (SEM) and the photocatalytic performance measurements via methyl orange (MeO) degradation under ultra-violet (UV) irradiation. Results showed that the most suitable TiO<sub>2</sub> catalyst had network shape.

**Keywords:** Photo catalysis, Synthesis, Two-dimensional structures

### Introduction

Increasingly serious ecological problems have attracted attention of researchers towards new catalytic techniques capable of removal or at least reduction in the daily emissions entering into the environment [1].

Photocatalytic semiconductors help acceleration of the decomposition reactions stimulated by light irradiation. Advanced oxidation process (AOP) is a means for decomposition of the organic-contaminants. It involves the following steps: (a) initial excitation, (b) electron-hole production, (c) free radicals participation and (d) recombination [2].

TiO<sub>2</sub> is a widely used semiconductor with valuable physicochemical properties, favorable band gap, low cost, chemical stability and nontoxicity [3,4]. It is known that TiO<sub>2</sub> is an n-type semiconductor with a band gap of 3.2eV located in the ultraviolet (UV) range [5]. The photocatalytic activity of titania depends on crystallinity, size and phase of crystallite, specific surface area and pore structure [6].

Nanoparticles of zero dimension, one-dimensional nanowires and nanotubes, two-dimensional nanosheets, three-dimensional mesoporous structures and nanonetworks have been studied by different researchers for specific applications. Among these, nanonetworks have absorbed particular attention because of large porosity and free surfaces which allow robust interaction with the solvent and solute molecules. Interconnected intact structure of the nanonetworks which extends from millimeter to centimeter lengths provides practical applicability in designing of the intricate devices [7].

This work concentrates on the effect of geometry of catalyst on methyl orange (MeO) decolorization under ultra violet (UV) light irradiation catalyzed by TiO<sub>2</sub> powder, fiber, film and networked geometries. From MeO color change, the photocatalytic activity of different samples was estimated. Decolorization of MeO by UV irradiation in presence of TiO<sub>2</sub> was verified by UV-vis

concentration measurements of the azo dye organic pollutant. Catalysts were characterized by XRD and SEM and compared for their catalytic behavior.

### Materials and method

Titanium (IV) isopropoxide (TTIP), hydrochloric acid (HCl), 2-propanol and methyl orange (MeO) were purchased from MERCK manufacturer. Distilled water, cellulose fibers and ceramic templates were obtained from local sources.

*Coprecipitation:* Distilled water (85cc), conc. HCl (6cc) and 2-propanol (6cc) were mixed and stirred together at the room temperature. After thorough mixing, titanium isopropoxide (5cc) was gradually added to the solution by a pipette. When the solution became clear, its temperature was slowly elevated to 333K by immersing its container into a water bath of controlled temperature. The substrate (cellulose fibers or ceramic template) were then dipped into the solution and left overnight to allow precipitation of a TiO<sub>2</sub> layer. The sample was then washed with deionized water and dried under air. For calcination of the sample, it was heated at 723K for 2h.

*TiO<sub>2</sub> characterization:* X-ray diffractometer (type D-64295) with Cu K<sub>α</sub> was used to determine the XRD patterns of the samples. SEM (LEO-1450VP) was used for morphological investigation of the samples.

*Photocatalytic degradation:* Catalytic activity of the samples was estimated from color degradation of the methyl orange aqueous solution (60cc MeO of 10 mg/L initial concentration). Before irradiation with UV light, the aqueous solution which contained MeO and TiO<sub>2</sub> catalyst was continuously stirred for 1h in full darkness to achieve adsorption-desorption equilibrium. UV irradiation from two 6W lamp (Philips, China) was then applied to the catalyst containing solution. The distance

between the surface of the solution and the light source was ~10cm. Samples were then taken out for analysis, every 30min.

MeO concentration was determined by UV-vis spectrophotometer (Jenway-6705). The maximum absorption wavelength registered was 462nm. The efficiency of degradation ( $\eta\%$ ) was calculated from the following equation [1]:

$$\eta\% = \left( \frac{C_0 - C}{C_0} \right) \times 100 \quad (1)$$

Where  $C_0$  and  $C$  are initial and at-time- $t$  concentrations of the dye, respectively.

### Results and Discussion

Fig. 1 shows XRD pattern of the produced  $\text{TiO}_2$ . Based on peaks of this pattern, anatase and rutile are the only phases present in the sample. Using the Scherer equation, the average crystallite sizes of anatase and rutile were estimated to be 21 and 19nm, respectively.

The fraction of the crystalline phases was determined by integrating the relative intensities of the anatase (101) ( $2\theta=25.4^\circ$ ) and the rutile (110) ( $2\theta=27.5^\circ$ ) peaks [8]:

$$W_R = \frac{A_R}{0.88A_A + A_R} \quad (2)$$

Where  $W_R$  is the weight fraction of the rutile and  $A_A$  and  $A_R$  represent the integrated intensities of the anatase (101) and the rutile (110) peaks, respectively. From Eq. 2, the fraction of the rutile in our samples was 0.27.

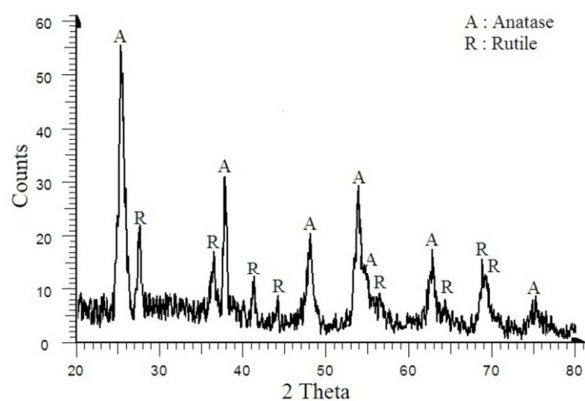


Fig. 1: XRD pattern of  $\text{TiO}_2$  powder calcined at 723K for 2h.

SEM images of  $\text{TiO}_2$  samples produced in this research are shown in Fig. 2. Particles shown in Fig. 2a have near-spherical agglomerated shape in the size range of 20-30nm.  $\text{TiO}_2$  microfibers shown in Fig. 2b are 30 $\mu\text{m}$  long hollow cylinders having 0.5-1 $\mu\text{m}$  diameters. They were produced by template-coating and removal of the cellulose base by subsequent heat treatment. The tubes have open ending. Energy dispersive x-ray (EDX) analysis of the fibers shown in Fig. 2c indicates Ti and O

presence in the annealed samples. SEM image of the  $\text{TiO}_2$  film is shown in Fig. 2d.

Fig. 3 illustrates network shape  $\text{TiO}_2$  catalyst. Particles deposited on wall of the substrate are highlighted.

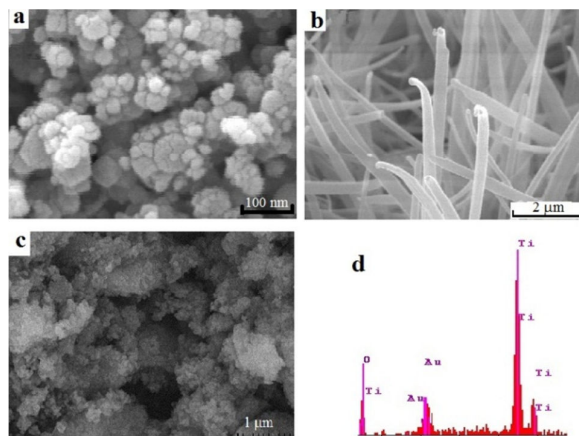


Fig. 2: SEM images of  $\text{TiO}_2$  (a) powder, (b) fiber and (c) film samples. EDX diagram of fibers is shown in (d).

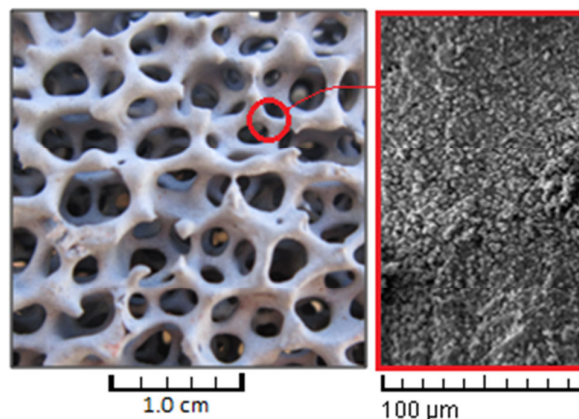


Fig. 3: Image of the  $\text{TiO}_2$  network sample.

Results for the degradation tests were determined as a function of the irradiation time ( $t$ ):

$$\ln\left(\frac{C_0}{C}\right) = kt \quad (3)$$

Where  $C_0$  and  $C$  are concentrations at start and after time  $t$  of the MeO dye. Fig. 4 compares the  $(C_0/C)$  ratio against time for different catalysts with and without UV irradiation. A pseudo-first order kinetic model (Eq. 3) was applied to compare the degradation performance of different catalysts and no UV tests. The plot of  $\ln(C_0/C)$  versus  $t$  was close to linear for all experiments (Fig. 5). Degradation rate constant  $k$  of the MeO dye was obtained by regression analysis of the data given in Fig. 5. Same initial concentrations of MeO were used to obtain data of

Fig. 5. Effect of TiO<sub>2</sub> geometry on efficiency of the MeO degradation is shown in Fig. 6.

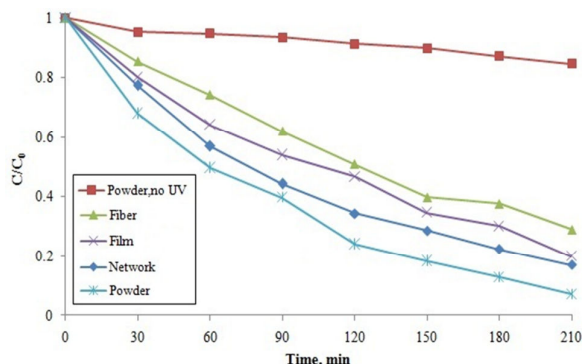


Fig. 4. MeO degradation dependence on structure of the TiO<sub>2</sub>.

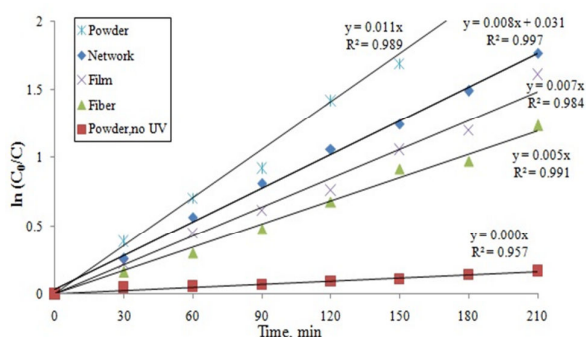


Fig. 5. First order kinetic plots of the MeO photodegradation in presence of different catalysts.

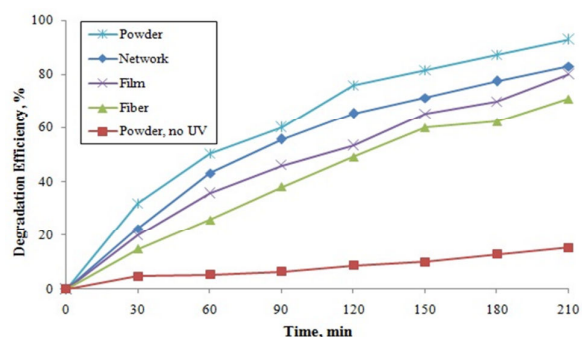


Fig. 6. Comparison of MeO degradation for different catalysts and no UV irradiation.

According to Figs. 4 to 6, the powdery sample yields the highest degradation. Its use is not, however, desirable; because its collection after utilization is a total mess. Powdery catalysts move with the solution and cannot be removed from the reaction environment. Film and fiber

shapes have less reaction surfaces as compared to the network structure. Network geometry is hence the most suitable TiO<sub>2</sub> catalyst shape. It has all advantages of production simplicity, environmental stability and high catalytic performance.

## Conclusions

In this work, four geometries of TiO<sub>2</sub> (powder, fiber, film and network) were produced by coprecipitation from a synthesized raffinate. Morphologies of the samples were determined from their SEM images. Their photocatalytic properties were determined and from MeO degradation data obtained from color change and solution composition alteration. The network geometry was introduced as the most desirable TiO<sub>2</sub> catalyst shape.

## References

- [1]. A.R. Khataee, M. Zarei, S. Khameneh Asl, "Photocatalytic treatment of a dye solution using immobilized TiO<sub>2</sub> nanoparticles combined with photoelectro-Fenton process: Optimization of operational parameters", *Electroanalytical Chemistry*, 648 (2010) 143-150.
- [2]. J.H. Kim, G. Seo, D.L. Cho, B.C. Choi, "Development of air purification device through application of thin-film photocatalyst", *Catalysis Today*, 111 (2006), 271-274.
- [3]. B. Tian, Z. Shao, Y. Ma, J. Zhang, F. Chen, "Improving the visible light photocatalytic activity of mesoporous TiO<sub>2</sub> via the synergetic effects of B doping and Ag loading", *Physics and Chemistry of Solids*, 72 (2011), 1290-1295.
- [4]. S. Khameneh Asl, M. Keyanpour Rad, S.K. Sadrnezhaad, M.R. Vaezi, "The Effect of Microstructure on the Photocatalytic Properties of TiO<sub>2</sub>", *Advanced Materials Research*, 264-265 (2011), 1340-1345.
- [5]. Y. Yang, Q. Zhang, B. Zhang, W. B. Mi, L. Chen, "The influence of metal interlayers on the structural and optical properties of nano-crystalline TiO<sub>2</sub> films", *Applied Surface Science*, 258 (2012), 4532-4537.
- [6]. J. Yu, Y. Su, B. Cheng, M. Zhou, "Effects of pH on the microstructures and photocatalytic activity of mesoporous nanocrystalline titania powders prepared via hydrothermal method", *Molecular Catalysis A: Chemical*, 258 (2006), 104-112.
- [7]. H. Ceylan, C. Ozgit-Akgun, T. S. Erkal, I. Donmez, "Size-controlled conformal nanofabrication of biotemplated three-dimensional TiO<sub>2</sub> and ZnO nanonetworks", *Scientific Reports*, 3:2306, (2013).
- [8]. Y. V. Kolenko, V. D. Maximov, A. V. Garshev, P. E. Meskin, N. N. Oleynikov, "Hydrothermal synthesis of nanocrystalline and mesoporous titania from aqueous complex titanyl oxalate acid solutions", *Chemical Physics Letters*, 388 (2004), 411-415.